EPJ A
Hadrons and Nuclei
EPJ.org
your physics journal

Eur. Phys. J. A (2011) **47**: 160 DOI 10.1140/epja/i2011-11160-x

Measurement of the neutron-induced fission cross-section of ^{243}Am relative to ^{235}U from 0.5 to 20 MeV

F. Belloni, M. Calviani, N. Colonna, P. Mastinu, P.M. Milazzo, U. Abbondanno, G. Aerts, H. Álvarez, F. Alvarez-Velarde, S. Andriamonje, J. Andrzejewski, L. Audouin, G. Badurek, M. Barbagallo, P. Baumann, F. Bečvář, E. Berthoumieux, F. Calviño, D. Cano-Ott, R. Capote, C. Carrapiço, P. Cennini, V. Chepel, E. Chiaveri, G. Cortes, A. Couture, J. Cox, M. Dahlfors, S. David, I. Dillmann, C. Domingo-Pardo, W. Dridi, I. Duran, C. Eleftheriadis, M. Embid-Segura, A. Ferrari, R. Ferreira-Marques, K. Fujii, W. Furman, I. Goncalves, E. Gonzalez-Romero, A. Goverdovski, F. Gramegna, C. Guerrero, F. Gunsing, B. Haas, R. Haight, M. Heil, A. Herrera-Martinez, M. Igashira, E. Jericha, F. Käppeler, Y. Kadi, D. Karadimos, D. Karamanis, M. Kerveno, P. Koehler, E. Kossionides, M.

Krtička, C. Lamboudis, H. Leeb, A. Lindote, I. Lopes, M. Lozano, S. Lukic, J. Marganiec, S. Marrone, T. Martínez, C. Massimi, M.H. Meaze, A. Mengoni, C. Moreau, M. Mosconi, F. Neves, H. Oberhummer, S. O'Brien, J. Pancin, C. Papachristodoulou, C. Papadopoulos, C. Paradela, N. Patronis, A. Pavlik, P. Pavlopoulos, L. Perrot, M.T. Pigni, R. Plag, A. Plompen, A. Plukis, A. Poch, J. Praena, C. Pretel, J. Quesada, T. Rauscher, R. Reifarth, M. Rosetti, C. Rubbia, G. Rudolf, P. Rullhusen, J. Salgado, C. Santos, L. Sarchiapone, I. Savvidis, C. Stephan, G. Tagliente, J.L. Tain, D. Tarrio, L. Tassan-Got, L. Tavora, R. Terlizzi, G. Vannini, P. Vaz, A. Ventura, D. Villamarin, M.C. Vincente, V. Vlachoudis, R. Vlastou, F. Voss, S. Walter, M. Wiescher and K. Wisshak

Eur. Phys. J. A (2011) **47**: 160
DOI 10.1140/epja/i2011-11160-x

THE EUROPEAN PHYSICAL JOURNAL A

Regular Article – Experimental Physics

Measurement of the neutron-induced fission cross-section of ^{243}Am relative to ^{235}U from 0.5 to 20 MeV

F. Belloni[1], M. Calviani[2,3], N. Colonna[4], P. Mastinu[2], P.M. Milazzo[1,a], U. Abbondanno[1], G. Aerts[5], H. Álvarez[6], F. Alvarez-Velarde[7], S. Andriamonje[5], J. Andrzejewski[8], L. Audouin[9], G. Badurek[10], M. Barbagallo[4], P. Baumann[11], F. Bečvář[12], E. Berthoumieux[5], F. Calviño[13], D. Cano-Ott[6], R. Capote[14,15], C. Carrapiço[16], P. Cennini[3], V. Chepel[17], E. Chiaveri[3], G. Cortes[13], A. Couture[18], J. Cox[18], M. Dahlfors[3], S. David[11], I. Dillmann[9], C. Domingo-Pardo[19], W. Dridi[5], I. Duran[6], C. Eleftheriadis[20], M. Embid-Segura[6], A. Ferrari[3], R. Ferreira-Marques[17], K. Fujii[1], W. Furman[21], I. Goncalves[16], E. Gonzalez-Romero[6], A. Goverdovski[22], F. Gramegna[2], C. Guerrero[7], F. Gunsing[5], B. Haas[23], R. Haight[24], M. Heil[9], A. Herrera-Martinez[3], M. Igashira[25], E. Jericha[10], F. Käppeler[9], Y. Kadi[3], D. Karadimos[26], D. Karamanis[26], M. Kerveno[11], P. Koehler[27], E. Kossionides[28], M. Krtička[12], C. Lamboudis[20], H. Leeb[10], A. Lindote[17], I. Lopes[17], M. Lozano[29], S. Lukic[11], J. Marganiec[8], S. Marrone[4], T. Martínez[7], C. Massimi[30], M.H. Meaze[4], A. Mengoni[3,14], C. Moreau[1], M. Mosconi[9], F. Neves[17], H. Oberhummer[10], S. O'Brien[18], J. Pancin[5], C. Papachristodoulou[26], C. Papadopoulos[31], C. Paradela[6], N. Patronis[26], A. Pavlik[32], P. Pavlopoulos[33], L. Perrot[5], M.T. Pigni[27], R. Plag[9], A. Plompen[34], A. Plukis[5], A. Poch[13], J. Praena[29], C. Pretel[13], J. Quesada[29], T. Rauscher[35], R. Reifarth[24], M. Rosetti[36], C. Rubbia[37], G. Rudolf[11], P. Rullhusen[34], J. Salgado[16], C. Santos[16], L. Sarchiapone[3], I. Savvidis[20], C. Stephan[38], G. Tagliente[4], J.L. Tain[19], D. Tarrio[6], L. Tassan-Got[38], L. Tavora[16], R. Terlizzi[4], G. Vannini[30], P. Vaz[16], A. Ventura[36], D. Villamarin[7], M.C. Vincente[7], V. Vlachoudis[3], R. Vlastou[31], F. Voss[9], S. Walter[9], M. Wiescher[18], and K. Wisshak[9]

[1] Istituto Nazionale di Fisica Nucleare (INFN), Trieste, Italy
[2] Istituto Nazionale di Fisica Nucleare (INFN), Laboratori Nazionali di Legnaro, Italy
[3] CERN, Geneva, Switzerland
[4] Istituto Nazionale di Fisica Nucleare (INFN), Bari, Italy
[5] CEA, Irfu, Gif-sur-Yvette, France
[6] Universidade de Santiago de Compostela, Spain
[7] Centro de Investigaciones Energeticas Medioambientales y Technologicas, Madrid, Spain
[8] University of Lodz, Lodz, Poland
[9] Karlsruhe Institute of Technology, Campus Nord, Institut für Kernphysik, Germany
[10] Atominstitut der Österreichischen Universitäten, Technische Universität Wien, Austria
[11] Centre National de la Recherche Scientifique/IN2P3 - IReS, Strasbourg, France
[12] Faculty of Mathematics and Physics, Charles University in Prague, Czech Republic
[13] Universitat Politecnica de Catalunya, Barcelona, Spain
[14] International Atomic Energy Agency (IAEA), NAPC/Nuclear Data Section, Vienna, Austria
[15] Universidad de Sevilla, Spain
[16] Instituto Tecnológico e Nuclear (ITN), Lisbon, Portugal
[17] LIP - Coimbra & Departamento de Fisica da Universidade de Coimbra, Portugal
[18] University of Notre Dame, Notre Dame, USA
[19] Instituto de Física Corpuscular, CSIC-Universidad de Valencia, Spain
[20] Aristotle University of Thessaloniki, Greece
[21] Joint Institute for Nuclear Research, Frank Laboratory of Neutron Physics, Dubna, Russia
[22] Institute of Physics and Power Engineering, Obninsk, Russia
[23] Centre National de la Recherche Scientifique/IN2P3 - CENBG, Bordeaux, France
[24] Los Alamos National Laboratory, New Mexico, USA
[25] Tokyo Institute of Technology, Tokyo, Japan
[26] University of Ioannina, Greece
[27] Oak Ridge National Laboratory, Oak Ridge, USA
[28] NCSR, Athens, Greece
[29] Universidad de Sevilla, Spain
[30] Dipartimento di Fisica, Università di Bologna and Sezione INFN di Bologna, Italy
[31] National Technical University of Athens, Greece

[a] e-mail: paolo.milazzo@ts.infn.it

[32] Institut für Fakultät für Physik, Universität Wien, Austria
[33] Pôle Universitaire Léonard de Vinci, Paris La Défense, France
[34] CEC-JRC-IRMM, Geel, Belgium
[35] Department of Physics and Astronomy, University of Basel, Switzerland
[36] ENEA, Bologna, Italy
[37] Università degli Studi di Pavia, Pavia, Italy
[38] Centre National de la Recherche Scientifique/IN2P3 - IPN, Orsay, France

Received: 5 July 2011 / Revised: 7 December 2011
Published online: 22 December 2011

Communicated by C. Signorini

Abstract. The ratio of the neutron-induced fission cross-sections of ^{243}Am and ^{235}U was measured in the energy range from 0.5 to 20 MeV with uncertainties of ≈4%. The experiment was performed at the CERN n_TOF facility using a fast ionization chamber. With the good counting statistics that could be achieved thanks to the high instantaneous flux and the low backgrounds, the present results are useful for resolving discrepancies in previous data sets and are important for future reactors with improved fuel burn-up.

1 Introduction

Nuclear energy may play an important role in future as part of the global energy mix. This energy source is critical to correct the world's energy imbalance, with 1.6 billion people not having access to electricity as an essential commodity for development. Many of the new power reactors now being constructed are located in developing countries and in China. The importance of nuclear power is also related to the fact that the reduction of CO_2 emission responsible for the greenhouse effect is currently a worldwide objective. Energy from nuclear reactors, in conjunction with renewable energy sources, may allow to achieve this goal.

On the other hand, there are a number of concerns that need to be addressed in the areas of nuclear safety, security, and non-proliferation. Most importantly, a reduction of the high-level nuclear waste is a fundamental pre-requisite for public acceptance of this energy source. Among the long-lived transuranium isotopes in the nuclear waste, the minor actinide (MA) isotope ^{243}Am plays an important role, because it contributes to the long-term production of ^{239}Pu via α- and subsequent β-decay.

Advanced Generation-IV reactors based on fast neutron spectra could be used to close the fuel cycle by minimizing the production of MAs via neutron-induced fission. The development of such reactors requires an accurate and consistent knowledge of neutron-induced fission cross-sections of heavy nuclei over a wide energy range. In a comparison of uncertainties quoted for evaluated data and the target accuracy assessment for innovative systems [1,2], it was found that accuracies of 2% and 7% for the ^{243}Am(n, *f*) cross-section are required for the development of a Sodium-cooled Fast Reactor (SFR) and for Advanced Minor Actinides Burner (ADMAB), respectively.

Existing experimental data have been obtained in a number of measurements [3–12]. However, severe discrepancies among these data are limiting the accuracy of evaluated data files to ≈10%. Unrecognized systematic uncertainties, *e.g.*, due to the α activity of the sample isotopic impurities, could be possible reasons for the large differences between previous results. Apart from the careful discussion of systematic effects, the present experiment has the advantage of covering a wide range of neutron energies with very good resolution, an aspect that is particularly important in view of the fission threshold of ^{243}Am near 0.5 MeV.

An extensive measurement campaign for reducing the uncertainties of the fission cross-section of ^{243}Am has been carried out at the neutron time-of-flight facility n_TOF at CERN, taking advantage of very high instantaneous neutron flux and extremely low duty cycle, which allows one to minimize the background related to the α activity of the sample. The present work focuses on the fission cross-section of ^{243}Am in the energy range from 500 keV to 20 MeV. The experiment is described in sect. 2, followed by the data analysis procedure in sect. 3. The extracted cross-section and the comparison to previous data are presented in sect. 4.

2 Experiment

2.1 Characteristics of the neutron beam

The measurement was performed at CERN using the pulsed neutron beam of the n_TOF facility. Neutrons are generated by means of spallation reactions on a massive lead target, induced by a high-energy proton beam (20 GeV), with high intensity (7×10^{12} protons per bunch), short pulse width (6 ns), and low duty cycle (1 pulse every 2.4 s) [13]. In particular, the combination of the high instantaneous flux of 10^5 neutrons/cm^2/pulse at the sample position and the extremely low duty factor of the n_TOF facility are instrumental for the strong reduction of the background related to the high α activity of the sample.

The spallation target itself in combination with a 5.8 cm thick layer of cooling water surrounding it acts as moderator for the spallation neutrons. The experimental area at a distance of 187 m is connected with the target by an evacuated flight path with two collimators at 137 and 176 m. The various backgrounds components are suppressed by a 1.5 T sweeping magnet, heavy concrete walls, and a 3.5 m thick iron shielding located along the beam line [14]. The beam line extends 12 m beyond the experimental area to minimize the effect of back-scattered neutrons.

2.2 The experimental setup

The measurement has been carried out with a setup consisting of a stack of 16 fast ionization chambers in a common housing, thus allowing the simultaneous measurement on several isotopes [15]. Each chamber is made of a central Al cathode 100 μm in thickness plated on both sides with sample material, and two 15 μm thick Al anodes at a distance of 5 mm from the cathode for the definition of the electric field. The electrodes are 12 cm in diameter, while the sample deposit itself is 8 cm in diameter to match the size of the neutron beam. The detector setup is operated with a gas mixture of 90% Ar and 10% CF_4 at a pressure of 720 mbar.

The samples were prepared by means of the painting technique. The eight ^{243}Am samples consisted of material with 97.0% enrichment in ^{243}Am and an ^{241}Am admixture of 2.6%, whereas the two ^{235}U reference samples were made from almost isotopically pure material (99.992% ^{235}U). The α activity of the Am samples was of 7.390 MBq. More information on the samples used in the present measurement are given in table 1.

The long flight path between the spallation target and the experimental area assures high-resolution incident neutron energy determinations. Fission events were detected via the energy deposited in the gas by the fission fragments exiting the very thin layers of fissile material.

The detector signals were recorded using the standard n_TOF data acquisition system based on fast digitizers with a sampling rate of 100 MSamples/s [16].

Table 1. Characteristics of the samples used in the ^{243}Am(n,f) measurement; the ^{235}U sample has been used as reference.

Sample	Chemical form	Mass (mg)	Thickness (μg/cm^2)	Uncertainty (%)
^{243}Am	AmO_2	0.556	11.1	1.2
^{243}Am	AmO_2	0.585	11.6	1.2
^{243}Am	AmO_2	0.613	12.2	1.3
^{243}Am	AmO_2	0.631	12.5	1.3
^{243}Am	AmO_2	0.537	10.7	1.2
^{243}Am	AmO_2	0.558	11.1	1.2
^{243}Am	AmO_2	0.595	11.8	1.3
^{243}Am	AmO_2	0.710	14.1	1.2
^{235}U	U_3O_8	15.2	303	1.4
^{235}U	U_3O_8	16.6	330	1.3

3 Data analysis, corrections and uncertainties

For each fission event, the first step in data analysis consists in the off-line determination of the energy deposited in the detector by the fission fragments as well as their TOF.

In order to correct for absorption losses in the samples and for the threshold effect imposed by the α activity, realistic Monte Carlo simulations of the detector response were performed [15] with the FLUKA code [17]. The kinetic energy and mass of the fission fragments were randomly generated according to the respective distributions [18]. Energy losses by α particles and fission fragments in the gas volume and in the sample were carefully investigated, showing that the distribution of deposited fragment energy is well separated from the α background, as shown in fig. 1. The simulations showed also that the detector works properly if the event rate is lower than ≈65 MHz [15]. Because the total α activity of ^{243}Am is a factor of 10 lower than this limit, pile-up effects are very small in this measurement.

The experimental distributions are well reproduced by the simulations [15,19]. In particular, defining a lower threshold of 20 MeV in the deposited energy spectrum allows one to remove completely the α component from the measured fission yields.

The neutron energy associated with a fission event was extracted using the TOF energy relation provided by the calibration of ref. [20], which is based on the neutron production mechanism in the spallation target and the subsequent moderation process [14]. The length of the flight path was obtained by means of the analysis of the well-known ^{235}U resonances [20].

The ^{243}Am(n,f) cross-section has been extracted relative to the ^{235}U(n,f) cross-section, which is an established standard in the neutron energy range from 0.15 to 200 MeV [21], according to the following expression:

$$\sigma_{243}(n,\ f) = c(E_n) \cdot \sigma_{235}(n,\ f) \cdot \frac{N_{243}}{N_{235}} \cdot \frac{m_{235}}{m_{243}} \cdot \frac{A_{243}}{A_{235}}. \quad (1)$$

Here c is a correction factor depending on the incident neutron energy (E_n) that combines the detection efficiencies and dead-time effects, and $\sigma_{235U}(n,\ f)$ is the tabulated ENDF/B-VII.0 version of the ^{235}U(n,f) cross-section [22,23]. N denotes the number of detected fission events, m the sample mass, and A the atomic mass of considered isotope.

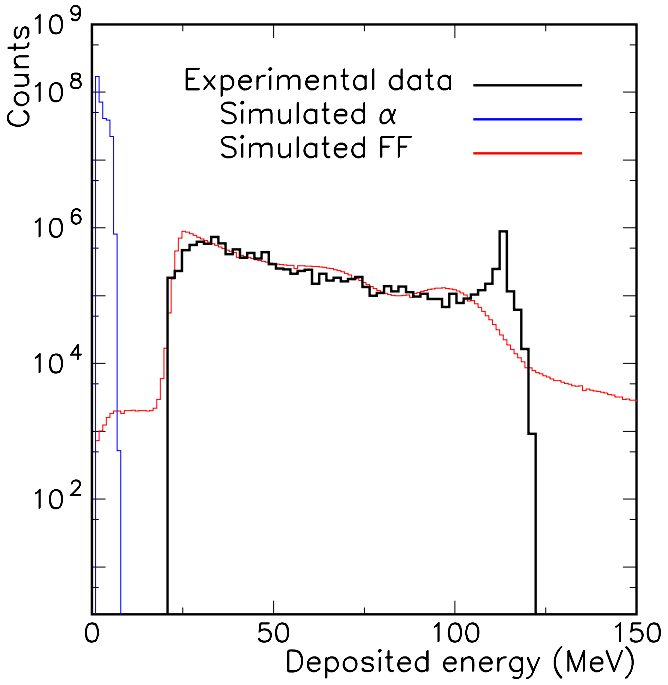

Fig. 1. (Color online) Comparison between the measured pulse height distribution (thick line) and the simulated spectrum for ^{243}Am indicating the α particle background at low energies and the response to fission fragments (thin lines). The difference between measurement and simulation is due to saturation effects in the detector above 100 MeV. The measured part is truncated at 20 MeV corresponding to the threshold adopted in the analysis.

Both samples were exposed to the same neutron flux and were measured with very similar detectors showing nearly identical efficiencies and signal shapes. Therefore, the application of the ratio method in comparison with a direct measurement has the significant advantage of minimizing the systematic uncertainties, especially with respect to the determination of the neutron flux.

The detector response to the ^{243}Am and ^{235}U samples differs slightly due to differences in sample thickness, which affects the detection efficiency, and in the count rate, which leads to slightly different dead-time and pile-up corrections. These differences are of the order of a few percent and must be carefully evaluated for an accurate cross-section determination. These sample-related corrections are expressed as

$$c = \frac{\varepsilon_{235} \cdot d_{235}}{\varepsilon_{243} \cdot d_{243}}, \quad (2)$$

where ε represents the efficiency for the detection of fission fragments and d the loss of counts due to dead time and pile-up.

Table 2. The cross-section ratio $\sigma(^{243}\mathrm{Am})/\sigma(^{235}\mathrm{U})$ and the deduced $^{243}\mathrm{Am}(n,\ f)$ cross-section in the neutron energy range between 0.5 and 20 MeV and the respective total uncertainties.

Energy bin (MeV)	$^{243}\mathrm{Am}(n,\ f)/^{235}\mathrm{U}(n,\ f)$	$^{243}\mathrm{Am}(n,\ f)$ (b)
0.501–0.562	0.0789 ± 0.006	0.0894 ± 0.007
0.562–0.631	0.0981 ± 0.007	0.110 ± 0.008
0.631–0.708	0.160 ± 0.009	0.18 ± 0.01
0.708–0.794	0.246 ± 0.01	0.27 ± 0.01
0.794–0.891	0.428 ± 0.02	0.48 ± 0.02
0.891–1.000	0.748 ± 0.03	0.88 ± 0.03
1.00–1.12	1.05 ± 0.04	1.25 ± 0.04
1.12–1.26	1.15 ± 0.04	1.38 ± 0.05
1.26–1.41	1.18 ± 0.04	1.44 ± 0.05
1.41–1.58	1.24 ± 0.04	1.52 ± 0.05
1.58–1.78	1.17 ± 0.04	1.46 ± 0.05
1.78–2.00	1.14 ± 0.04	1.44 ± 0.05
2.00–2.24	1.14 ± 0.04	1.45 ± 0.05
2.24–2.51	1.16 ± 0.04	1.46 ± 0.05
2.51–2.82	1.18 ± 0.04	1.46 ± 0.05
2.82–3.16	1.24 ± 0.04	1.49 ± 0.05
3.16–3.55	1.30 ± 0.05	1.52 ± 0.06
3.55–3.98	1.30 ± 0.05	1.49 ± 0.06
3.98–4.47	1.30 ± 0.05	1.45 ± 0.06
4.47–5.01	1.37 ± 0.06	1.49 ± 0.06
5.01–5.62	1.43 ± 0.06	1.50 ± 0.06
5.62–6.31	1.54 ± 0.05	1.68 ± 0.07
6.31–7.08	1.44 ± 0.06	2.05 ± 0.09
7.08–7.94	1.36 ± 0.06	2.31 ± 0.09
7.94–8.91	1.23 ± 0.05	2.19 ± 0.09
8.91–10.00	1.19 ± 0.05	2.09 ± 0.09
10.00–11.22	1.26 ± 0.05	2.18 ± 0.09
11.22–12.59	1.27 ± 0.06	2.20 ± 0.1
12.59–14.13	1.26 ± 0.06	2.46 ± 0.1
14.13–15.85	1.18 ± 0.05	2.46 ± 0.1
15.85–17.78	1.05 ± 0.05	2.15 ± 0.1
17.78–19.95	1.20 ± 0.05	2.33 ± 0.1

The detection efficiency depends essentially on the sample thickness and on the 20 MeV threshold for the deposited energy. From the Monte Carlo simulations described above, the efficiencies were found to be 99.7% and 95.1% for ^{243}Am and for the thicker ^{235}U sample, respectively. The resulting efficiency correction is 4.6%.

With the data acquisition system used at n_TOF, which is based on flash ADCs [16], dead-time problems are strongly reduced. However, a small effect persists because the signal reconstruction routine operates with a resolution time of 270 ns. The necessary corrections have been evaluated by means of a non-paralyzable model, where the instantaneous count rate was determined for each sample as a function of neutron energy. Average dead-time corrections are 5%, with a maximum of 10% at 2 MeV neutron energy.

The overall uncertainty of the present $^{243}\mathrm{Am}(n,f)$ cross-section includes also contributions related to the sample masses, to the $^{235}\mathrm{U}(n,f)$ cross-section, to the beam energy resolution, and to the counting statistics. The determination of the sample masses by α spectroscopy leads to an uncertainty of 1.9% with almost equal contributions of 1.3% and 1.35% from ^{243}Am and ^{235}U, respectively. The uncertainty of the ^{235}U reference cross-section is typically 2% in the energy region of interest here [21], and the corrections for the detection efficiencies and dead-time effects are estimated to add uncertainties of the order of 1.0% each. For most of the energy range covered by the present analysis, the uncertainty in neutron energy is determined by the time resolution of the initial proton beam and increases from about 0.1% at 0.5 MeV to 0.6% at 20 MeV [14].

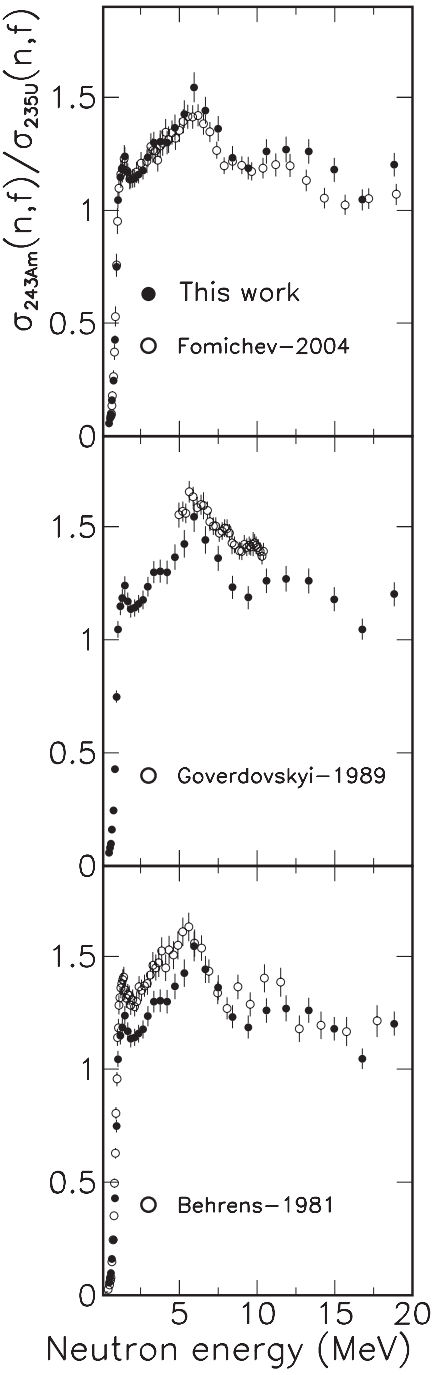

Fig. 2. Comparison of the present cross-section ratios $\sigma(^{243}\mathrm{Am})/\sigma(^{235}\mathrm{U})$ (solid points, 20 bins per energy decade) with previous measurements (open points) [5,6,10].

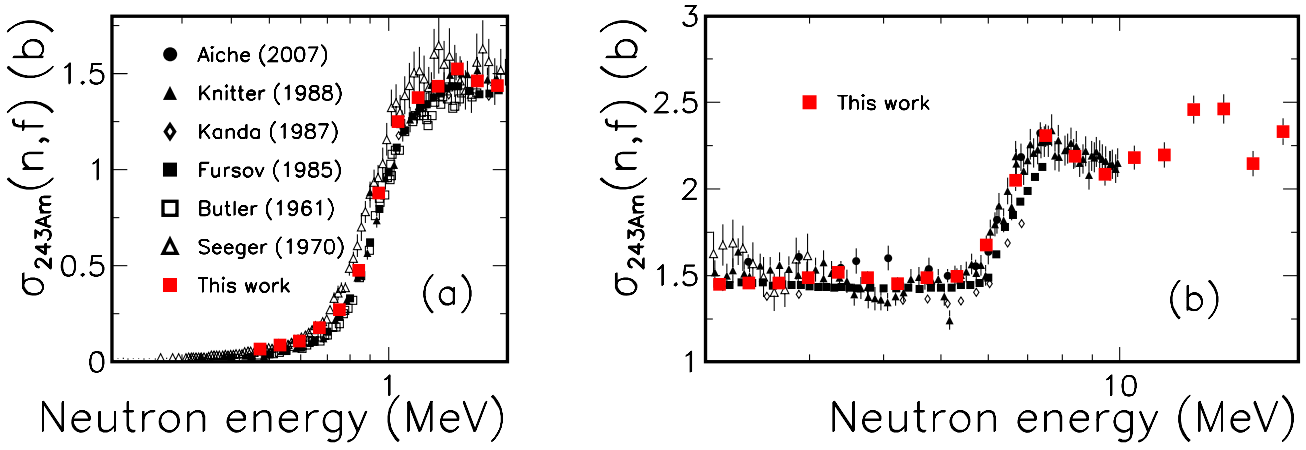

Fig. 3. (Color online) Comparison of present fission cross-section of ^{243}Am (full squares, 20 bins per energy decade) with previous measurements [3,7–9,11,12,23].

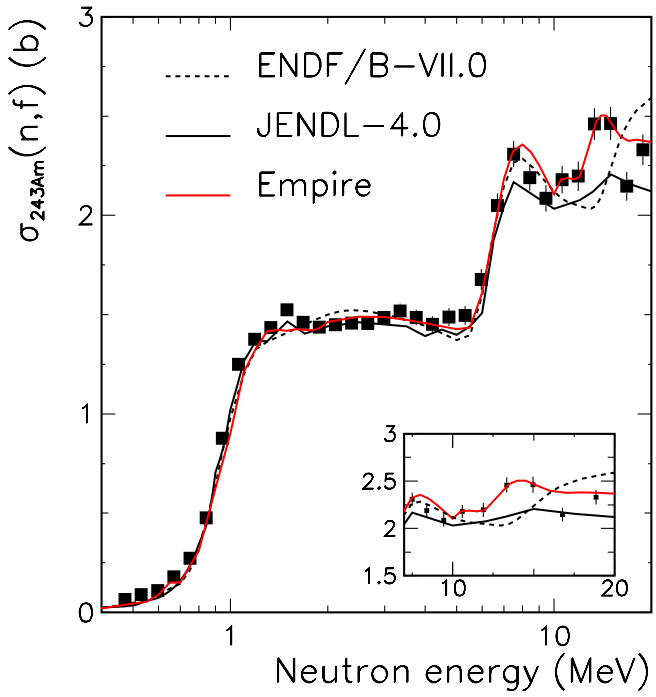

Fig. 4. (Color online) Comparison of present cross-section (full squares, 20 bins per energy decade) with the most recent evaluations [23–25].

The resulting systematic uncertainty of the ^{243}Am(n,f) cross-section is ≈3%. If the data are given with a resolution of 20 bins per energy decade, the statistical uncertainty per bin is also ≈3%, resulting in a total uncertainty of typically 4%.

4 Results

The neutron-induced fission cross-section of ^{243}Am was measured relative to that of ^{235}U in the energy range between 0.5 and 20 MeV. The corresponding cross-section ratios $\sigma(^{243}\text{Am})/\sigma(^{235}\text{U})$ and the final values for the ^{243}Am fission cross-section are summarized in table 2.

Table 3. Differences between the present and previous energy-integrated cross-sections in the energy range of overlap. Evaluated data are from ref. [23].

Authors	Ref.	Energy range (MeV)	Difference (%)
Aiche *et al.*	[3]	1.8–7.4	−3.9
Fomichev *et al.*	[5]	0.59–20.	+5.2
Goverdovskiy *et al.*	[6]	5.0–10.4	−11.9
Behrens and Browne	[10]	0.5–20.	−6.5
Seeger	[11]	0.5–3.	−6.3
ENDF/B-VII.0		1.–20.	+0.9
JENDL-4.0		1.–20.	+6.0
JEFF-3.1.1		1.–20.	+4.8
ROSFOND		1.–20.	+4.3
BROND-2.2		1.–20.	+3.6
Empire		1.–20.	−1.5

The present results are compared with previous data and evaluations in figs. 2, 3 and 4. Energy-integrated cross-sections in the region of overlap with previous data sets are compared in table 3.

4.1 Comparison with previous measurements

In some of the previous studies the ^{243}Am(n,f) cross-section has been obtained with the same technique as used in the present experiment [5,6,10], *i.e.* by measuring the cross-section ratio ^{243}Am$(n,f)/^{235}$U(n,f). To avoid systematic effects in the determination of the ^{243}Am(n,f) cross-section due to the ^{235}U(n,f) reference cross-section, the measured ^{243}Am$(n,f)/^{235}$U(n,f) ratios are directly compared in fig. 2.

Significant discrepancies of up to 20% are found with respect to the older cross-section ratios [6,10], while the present results are in good agreement with the data of Fomichev *et al.* [5], except for some differences above 10 MeV.

The absolute fission cross-section of ^{243}Am determined at n_TOF is compared with previous data given in refs. [3, 7–9,11,12,23] in fig. 3. We remind that in the present work the ^{235}U(n, f) cross-section from ENDF/B-VII.0 was used as reference to extract the absolute value from the measured cross-section ratios. The left panel of fig. 3 highlights the energy range of the fission threshold and the right panel covers the first fission plateau and the opening of the second-chance fission channel.

A general agreement is found with the previous measurements. However, differences are present in the energy scales introducing a broadening of the thresholds for the opening of the channels for first- and second-chance fission. In particular, the data of Seeger *et al.* [11] appear to be shifted by approximately 50 keV relative to the other experimental results. Good agreement is also found with the recent data of Laptev *et al.* [4]. Unfortunately, the information given for the ^{243}Am target used in that experiment is incomplete [23] so that the data can only be used for a comparison of the cross-section shape.

For those data sets showing a fair agreement in the cross-section shapes, the average differences to previous measurements are summarized in table 3 by comparison of the energy-integrated cross-sections over the energy range of overlap.

4.2 Comparison with evaluated data

The present results for the fission cross-section of ^{243}Am are compared in fig. 4 with the most recent evaluations from ENDF/B-VII.0 [23] and from JENDL-4.0 [24], as well as from a new evaluation performed with the nuclear reaction model code Empire [25]. The Empire code defines an optical model for fission, in approximation of partial damping, based on a two-humped barrier formalism. A more extended evaluation of neutron cross-sections of Am isotopes inside the framework of the Empire model, which will take into account also the new n_TOF data on ^{241}Am, is planned and will be described in detail elsewhere after completion.

Up to the threshold for second-chance fission there is very good agreement with all evaluations, but at higher energies only the Empire evaluation well reproduces present data. This is reflected in the comparison of table 3 by the larger difference of the energy-integrated cross-section of the JENDL case. We have to stress that, even though the ENDF/B-VII.0 evaluation presents the best result between those listed in table 3, this is an artifact due to the average of significant under and overestimations of the present fission cross-section above 10 MeV. In addition to the examples shown in fig. 4, the evaluated fission cross-section of ^{243}Am from all main data libraries [23] are included in table 3 as well.

5 Conclusions

The fission cross-section of ^{243}Am has been measured at the CERN n_TOF facility relative to that of ^{235}U. Results are reported in the energy range between 0.5 and 20 MeV with uncertainties of ≈4%. The possible systematic uncertainties due to sample masses, α backgrounds, detection efficiencies, and dead-time corrections were carefully considered.

For the fission cross-section ratio of ^{243}Am and ^{235}U, the present results are in good agreement with the most recent measurement [5]. This holds also for the deduced (n, f) cross-section of ^{243}Am, where the data of Aiche *et al.* are consistent with this measurement. However, it must be noted that there are differences in the energy range between 10 and 20 MeV, where the present data agree well only with the 30-year-old data of Behrens and Browne [10]. In summary, the present results suggest that a slight tuning of the evaluations for energies higher than 8 MeV seems to be in order.

This work was supported by the EC under contract FIKW-CT-2000-00107 and by the funding agencies of the participating institutes. The research leading to these results has received funding from the European Union's Seventh Framework Programme under the ANDES project, Grant Agreement n. 249671.

References

1. M. Salvatores, *Uncertainty and target accuracy assessment for innovative systems using recent covariance data evaluations*, Nucl. Sci., Vol. **26** (2008) available at `www.oecd-nea.org/html/science/wpec/volume26/volume26.pdf`.
2. G. Aliberti, G. Palmiotti, M. Salvatores, *NEMEA-4, Neutron measurements, evaluations and applications*, in *JRC Scientific and Technical Reports*, edited by A. Plompen (JRC, Belgium, 2008) p. 113.
3. M. Aiche, G. Kessedjian, G. Barreau, B. Jurado, A. Bidaud, S. Czajkowski, D. Dassie, B. Haas, L. Mathieu, L. Tassan-Got, J. Wilson, F.-J. Hambsch, S. Oberstedt, I. AlMahamid, J. Floyd, W. Lukens, D. Shuh, in *Proceedings of the International Conference on Nuclear Data for Science and Technology, April 22-27 2007, Nice, France*, edited by O. Bersillon, F. Gunsing, E. Bauge, R. Jacqmin, S. Leray (EDP Sciences, 2008) p. 483.
4. A.B. Laptev, A.Yu. Donets, V.N. Dushin, A.V. Fomichev, A.A. Fomichev, R.C. Haight, O.A. Shcherbakov, S.M. Soloviev, Yu.V. Tuboltsev, A.S. Vorobiev, A.D.Carlson, in *Proceedings of the Conference on Fission and Properties of Neutron-Rich Nuclei, Sanibel Island (2007)*, edited by J.H. Hamilton, A.V. Ramayya, H.K. Carter (World Scientific, 2008) p. 462.
5. A.V. Fomichev, V.N. Dushin, S.M. Soloviev, A.A. Fomichev, S. Mashnik, Khlopin Radiev. Inst., Leningrad Reports No. 262 (2004).

6. A.A. Goverdovskiy, A.K. Gordyushin, B.D. Kuz'minov, V.F. Mitrofanov, A.I. Sergachev, S.M. Solov'ev, T.E. Kuz'mina, At. Energ. **67**, 30 (1989).
7. H. Knitter, C. Budtz-Jorgensen, Nucl. Sci. Eng. **99**, 1 (1988).
8. K. Kanda, H. Imaruoka, H. Terayama, Y. Karino, N. Hirakawa, J. Nucl. Sci. Technol. **24**, 423 (1987).
9. B.I. Fursov, E.Ju. Baranov, M.P. Klemyshev, B.F. Samylin, G.N. Smirenkin, Yu.M. Turchin, At. Energ. **59**, 339 (1985).
10. J.W. Behrens, J.C. Browne, Nucl. Sci. Eng. **77**, 444 (1981).
11. P.A. Seeger, Los Alamos Sci. Lab. Rep. **4420**, 138 (1970).
12. D.K. Butler, R.K. Sjoblom, Phys. Rev. **124**, 1129 (1961).
13. C. Borcea *et al.*, Nucl. Instrum. Methods A **513**, 524 (2003).
14. The n_TOF Collaboration (U. Abbondanno *et al.*), CERN n_TOF facility: Performance report, Technical report CERNSL- 2002-053 ECT, CERN, Switzerland (2003).
15. M. Calviani *et al.*, Nucl. Instrum. Methods A **594**, 220 (2008).
16. The n_TOF Collaboration (U. Abbondanno *et al.*), Nucl. Instrum. Methods A **538**, 692 (2005).
17. A. Fassò, A. Ferrari, J. Ranft, P.R. Sala, Technical report CERN-2005-10, CERN, Switzerland (2005).
18. P. Hofmann *et al.*, Phys. Rev. C **49**, 2555 (1994) G.D. Adveev *et al.*, Preprint INR 816/93 (1993).
19. The n_TOF Collaboration (F. Belloni *et al.*), Eur. Phys. J. A **47**, 2 (2011).
20. The n_TOF Collaboration (G. Lorusso *et al.*), Nucl. Instrum. Methods A **532**, 622 (2004).
21. A.D. Carlson, V.G. Pronyaev, D.L. Smith, N.M. Larson, Zhenpeng Chen, G.M. Hale, F.-J. Hambsch, E.V. Gai, Soo-Youl Oh, S.A. Badikov, T. Kawano, H.M. Hofmann, H. Vonach, S. Tagesen, Nucl. Data Sheets **110**, 3215 (2009).
22. M.B. Chadwick *et al.*, Nucl. Data Sheets **107**, 2931 (2006).
23. For results compiled in evaluated nuclear data libraries see, for example, the *International Atomic Energy Agency (IAEA)* on `www-nds.iaea.org`, and the *OECD Nuclear Energy Agency* on `www.nea.fr/html/dbdata/`.
24. K. Shibata *et al.*, J. Nucl. Sci. Technol. **48**, 1 (2011).
25. M. Herman, R. Capote, B.V. Carlson, P. Obložinský, M. Sin, A. Trkov, H. Wienke, V. Zerkin, Nucl. Data Sheets **108**, 2655 (2007).